

# PREPARATION OF AERO TECHNOLOGY FOR NEW GENERATION AIRCRAFT ENGINE LP TURBINES

J. Gier, I. Raab, Th. Schröder,  
N. Hübner, M. Franke, F. Kennepohl,  
F. Lippl, T. Germain  
MTU Aero Engines GmbH  
Dachauer Str. 665, 80995 München  
Germany

Lars Enghardt  
German Aerospace Center (DLR)  
Institute of Propulsion Technology,  
Engine Acoustics Department  
Müller-Breslau-Str. 8, 10623 Berlin,  
Germany

## ABSTRACT

As flying becomes a more and more popular mean of transportation aero engines are faced with increased requirement concerning environmental issues and economic improvements. In order to achieve further steps into the direction of improved environmental friendliness and reduced operating costs MTU has been working on a large effort to improve future Low Pressure Turbines with respect to these issues. In this paper four large connected projects are described, which address turbine efficiency improvement, weight reduction, cost reduction and noise generation. In order to improve the turbine efficiency advanced 3D design through introduction of contoured endwalls has been developed. High lift airfoil design has been investigated as measure for a weight reduction. Thin solid airfoils have a cost benefit compared to hollow airfoils but the negative impact on the performance has to be minimized. And in order to significantly improve the noise prediction capability necessary for lower noise designs, specific acoustic tests have been performed. The paper describes the background of these topics and the steps taken to improve the technological basis. This is supported by discussing selected results.

## 1. INTRODUCTION

Modern aero engine turbines have to be designed and optimized with respect to several main targets. From an environmental point of view the turbine has to provide high efficiencies for low fuel burn and thus low CO<sub>2</sub> emissions. The weight of a jet engine is also directly related to the fuel burn, causing the need for light weight design. Another important environmental issue is the noise emission of jet engines. Since the LP turbine may be contributing to the overall noise to some extent it is important to explore ways for a further noise reduction. And finally the production and maintenance cost of a turbine has a significant impact on the economics of the aero engine.

To achieve improvements for these targets several solutions can be considered. However, quite often one solution, which aims for improvement with respect to one target, results in degradation with respect to other metrics. In order to improve the LP turbine design for new aero engines, several design options have been investigated within a large comprehensive project.

For each of the above mentioned main targets a sub-project has been defined and carried out. For efficiency

improvement the focus has been put on three-dimensional design of the flow path through airfoil rows focussing on non-axisymmetric endwall contouring.

Increased airfoil lift has been defined as measure for weight reduction, also contributing to cost reduction. Main focus of this project is to reduce the efficiency penalty for such designs.

For mainly cost reduction purpose thin solid airfoils are used in LP turbines. However, these also result in an efficiency decrease and this task is aiming at loss reduction for these thin airfoils. Finally the noise issue was addressed by considerable broadening the database for noise prediction and sensitivity analysis. For all main topics several investigation objects have been defined including full scale turbine rig testing.

## 2. IMPROVED 3D AERO DESIGN

Secondary flow is known to be a main driver of loss production in turbine blade rows. Due to the steep annulus and increased aerodynamic blade loading in modern low pressure turbines secondary loss can sum up to thirty percent of the total losses. The reduction of secondary loss is therefore essential in the struggle for further improvements in turbine efficiency.

The flow regime in a blade row is the result of the balance between the centrifugal flow forces and the blade pressure field. Near the endwalls the cross pressure gradient forces the slow fluid to deflect in the direction of the blade suction side, forming the so called passage vortex. Other vortex systems evolve due to the blockage of the blade leading edge and shear layers at the trailing edge (see FIG. 1). A good characterization of secondary flows is given in Langston et al. [1].

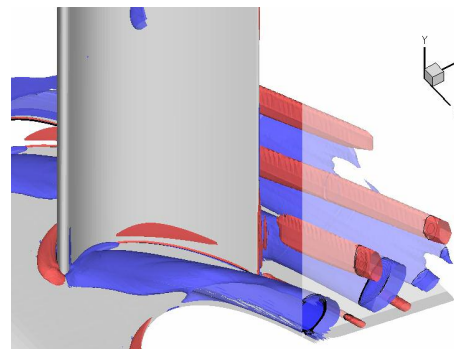


FIG. 1: Vortex system in airfoil passage

Measures to reduce the secondary losses address the design of geometries in order to influence the pressure field near the endwalls. Three-dimensional blade design was introduced to influence the spanwise pressure distribution by means of leaning and bowing the airfoils (e.g. Pioske [2]). The reduction of loading in the hub and tip regions is used to lower the excitation and the radial migration of the secondary flow. Other authors focused on the local modification of the blade by increasing the near wall airfoil sections (e.g. Duden et al. [3]) or the near end leading edge, Sauer et al. [4]. The resulting impact on the vortex system can beneficially influence the secondary flow.

A lot of different approaches to endwall design can be found in the open literature. Endwall contouring was first introduced as a measure to improve the secondary flow field for a given airfoil. Axisymmetric approaches (e.g. Pioske [2], Ardey and Gier [5], Eymann et al. [6], Gier et al. [7]) as well as non-axisymmetric designs (Harvey [8], Hartland [9], Rose [10], Nagel and Baier [11], Ingram [12]) have proved the potential to successfully reduce the secondary loss. With increasing numerical resources the aim of a 3D optimization of the entire flow path including airfoil, shroud and even the cavities becomes realistic for future engine design.

The benefit that can be derived by non-axisymmetric shroud contouring has recently become a major topic in the design of low pressure turbines. Therefore a project has been defined to systematically address the different aspects of the technology and to evaluate the potential of loss reduction for this specific application.

Due to the high complexity of the secondary flow system 3D numerical optimization has been chosen in this project as the adequate tool to deal with the great number of design parameters. The mathematical description of the endwalls is done with sinusoidal functions in axial and circumferential direction. The superposition of several functions allows for a great number of topology perturbations, Germain et al. [13].

Target functions and limiters have been tested with regard to their ability to create a successful design. A new definition of calculating the secondary kinetic energy (SKE) as described in [13] was used as the main target function for the optimization whereas the total loss is functioning as a limiter.

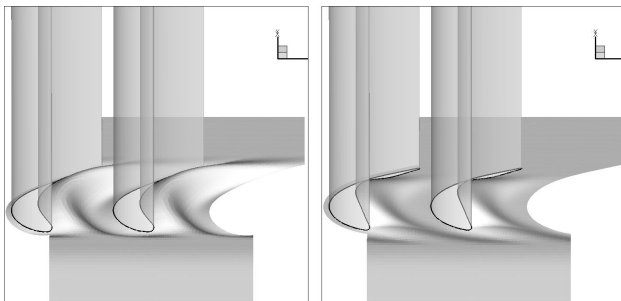


FIG. 2: Cascades T160A and T160B with contoured endwalls

The experimental evaluation has been done in three steps. Even with the use of numerical optimization the

underlying flow physics of the secondary flow and the resulting vortex system need to be studied numerically and experimentally for tool validation as well as for a better understanding of the design targets.

Firstly, two different types of endwall topologies have been tested in the high speed cascade wind tunnel of the University of the Armed Forces in Munich. The contoured endwalls applied to the test profile T160 can be seen in FIG. 2.

In a second step the design process was used for the design of contoured shrouds in two builds of the turbine test facility LISA at the ETH Zurich. In this case fillet radii have been treated as part of the endwall contour. The multi row environment gives additional insight into the interaction and downstream impact of secondary flow features. This test facility allows for detailed steady and unsteady aerodynamic measurements using five hole probes and FRAP sensors. A view of this 1.5-stage turbine is shown in Fig. 3 with more details given in Behr et al. [14, 15].

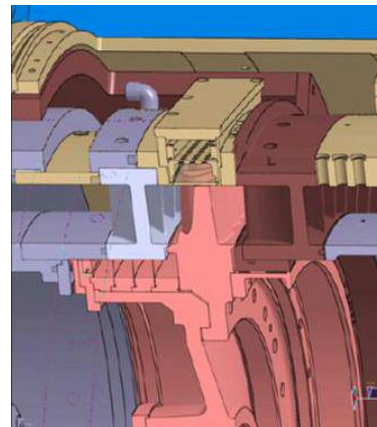


FIG. 3: View of 1 ½ stage turbine blading in ETH research turbine LISA (Behr et al. [14, 15])

The final experimental evaluation of the technology will be done with the test of a cold engine parts rig in the high altitude test facility at the University of Stuttgart later this year. In this case the technology has to prove applicability to an existing low pressure turbine. FIG. 4 shows a multicolour model of the topology of the first vane.



FIG. 4: First vane of cold flow rig with contoured endwalls

The described test series allows for a systematic study of the complex interaction between the geometry induced change in the local pressure field and the evolving secondary flow system.

First the design process had to be verified with respect to the optimization method and especially the target function focusing on the secondary kinetic energy SKE . FIG. 5 shows the good agreement between the predicted and the measured SKE in the reference and one of the contoured cascades. This supports the findings and assumptions of Rose et al. [10] that even if CFD may have problems in accurately predicting loss it shows good performance in terms of flow structure, hence secondary kinetic energy. Despite the different findings reported by Praisner et al. [16] the numerical prediction of the total pressure loss did not prove to be as reliable an indicator for loss reduction in the measurement.

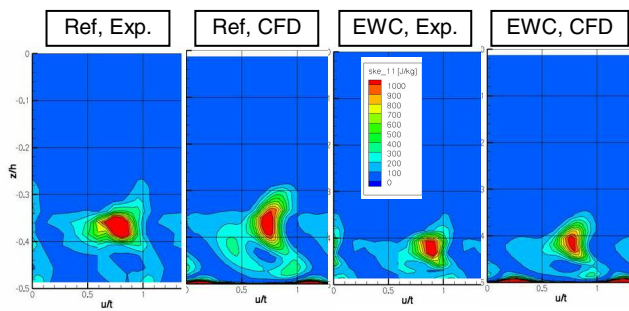


FIG. 5: Secondary kinetic energy for T160, test data and CFD for reference case (Ref.) and endwall contouring case (EWC) (Entlesberger [17])

The capability of the chosen method to find a loss reduced contoured design can be seen in FIG. 6 Even though the total pressure loss was no design target, the test data shows the reduced loss intensity in the measurement plane behind stator 1 of LISA 1. As a result the efficiency in the contoured turbine was significantly higher than in the non contoured case.

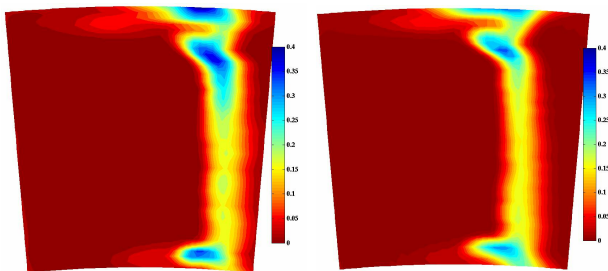


FIG. 6: Total pressure loss-coefficient downstream of the first stator in LISA 1, left baseline, right contoured (Schüpbach [18])

Summarizing the results gained so far it can be stated that an optimisation based design process has been established which was able to improve secondary flow losses in different applications. Due to the finding that fillet radii are an essential part of the shroud contour they have been included in the optimisation process. Further work is done on unsteady CFD-calculations to be validated against the unsteady test data.

### 3. HIGH LIFT AIRFOILS

The weight and cost of a low pressure turbine is considerably driven by the airfoil count. In typical LP turbines about half of the module weight is determined by the airfoils. Thus, reduction of the airfoil count directly influences the weight of the turbine component. In addition, lower airfoil count reduces the production and maintenance cost of the turbine. Unfortunately, low airfoil count results in an increased aerodynamic airfoil load. It is known, that depending on the boundary conditions of the airfoil row an optimum airfoil loading exists. Beyond this airfoil load the aerodynamic losses grow and efficiency is impaired. In terms of the design of an LP turbine it is absolutely necessary to be able to accurately predict the performance influence in order to trade this with the weight and cost savings.

The aerodynamic airfoil load is usually characterized by the dimensionless Zweifel coefficient, which is defined by the relationship between the area of the pressure distribution and the ideal area between total inlet pressure and static exit pressure. Usually high lift airfoils are referred to having Zweifel numbers larger than 1. Actually, MTU LP turbine designs in engines like the V2500, which entered service in the late 80's, already have airfoil rows with Zweifel coefficients in the order of 1 or somewhat higher. A good overview with respect to LP turbine aero design can be found in Hourmouziadis [19].

Later the concept of high lift design was studied in a much broader way. Schulte and Hodson [20] investigated high lift airfoils in conjunction with unsteadily impinging wakes in a cascade. It was demonstrated that the periodic fluctuations modelled by passing bars resulted in a stabilization of the boundary layer and reduced separation bubble size.

Gier et al. [21] and Ardey et al. [22] investigated differences between moderate and high lift 2<sup>nd</sup> vane in a three-stage LP turbine using transitional CFD for analysis. In Stadtmüller et al. [23] and Howell et al. [24] further investigations in cascades were performed with passing bars on high lift airfoils. Gier and Ardey [25] investigated the mechanism for the increasing loss due to high lift and based on this combined with radial rig traverse data Ardey and Gier et al. [26] investigated the effect of high lift on the 3D flow and the related losses.

Haselbach et al. [27] and Howell et al [28] introduced 2 high lift levels into the 3 stage LP turbine of the BR710 / 715 family. They reported that the Reynolds number lapse rate, hence efficiency drop at lower Reynolds numbers was significantly stronger for the so-called ultra high lift design with Zweifel numbers in the area of 1.1 to 1.2.

Houtermans and Coton [29] put additional focus on the separation prediction of high lift airfoils. Zhang et al. [30] and Vera et al. [31] investigated turbulation devices to be applied on the airfoil suction side in order to suppress large separation bubbles present in high lift airfoils in a low-speed and a high-speed facility, respectively. Popovic et al. [32] tested 2 airfoils with extremely high Zweifel numbers in the area of 1.4 in a low-speed cascade and Praisner et al. [33] investigated the performance improvement potential of contoured endwalls. Lazaro et

al. [34] took a close look into the loss production mechanism in a low-speed cascade with moving bars.

Based on the experience at MTU concerning high lift design and the literature available at the time a technology program has been started in order to develop a state-of-the-art high lift design and to explore options to limit the efficiency penalty. The project has 2 major steps, development and testing of two cascades with the same lift level but different airfoil shapes and a comprehensive full LP turbine rig test .

The cascades investigated are shown in FIG. 7. The 2 high lift cascades have been designed for the same velocity triangle as the baseline airfoil T160 with a lift increase of around 25%. All cascades have been measured without and with unsteady bar passing for impinging wake modelling.

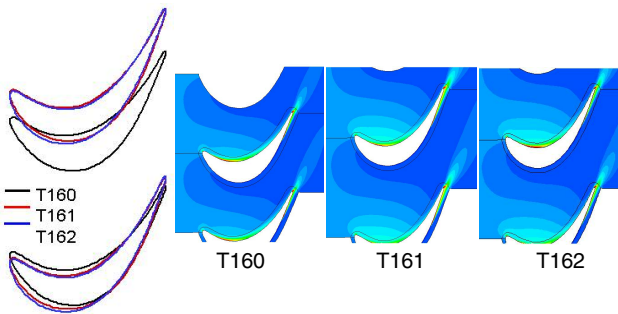


FIG. 7: Comparison of high lift cascades with conventional cascade, geometry and CFD comparison of turbulence intensity

In FIG. 8 the variation of the loss coefficient vs. Reynolds number is shown for both the steady and the unsteady case. In the steady case it becomes obvious that the two different high lift airfoil designs have a quite different characteristic. While the T161 shows a strong loss increase for the lower Reynolds numbers it achieves similar loss levels at Reynolds numbers between 200,000 and 400,000 as the baseline T160 cascade. In contrast the T162, which was designed for lower Reynolds numbers, exhibits a very comparable loss level as the baseline airfoil. Only at the lower end of the investigated Reynolds number range some limited loss increase can be found.

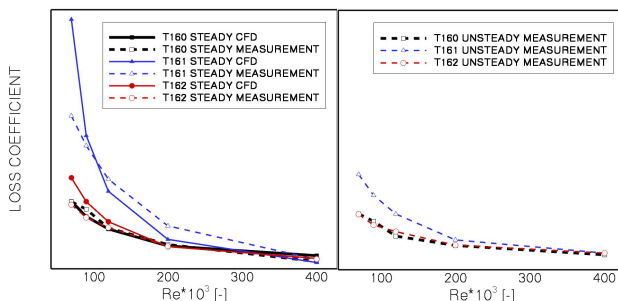


FIG. 8: Comparison loss coefficients of high lift cascades with conventional cascade, midspan results

These configurations have also been computed with CFD in order to test the current modelling capabilities including transition modelling. It can be stated that the main trend is well captured. However, there still exist some deviations, especially in the case of the T161, which has the more aggressive suction side pressure distribution. When the moving bars are present, the loss Reynolds lapse rate is significantly altered. The T161 still has increased losses in the lower Reynolds number regime, but the difference is significantly reduced. This again demonstrates the strong influence of the wake-unsteadiness in LP turbines.

These cascade test results are used for further CFD improvement and were the basis for the airfoil design in the five-stage engine-like turbine rig. In order to assess the performance impact of the high lift design on efficiency an existing full-scale five-stage rig has been modified in 7 of the 10 airfoil rows. FIG. 9 shows the general arrangement of the rig. The modified airfoils are marked in blue. The rig was heavily instrumented with several traverses also inside the rig. This was done in order to gain information not only for the entire turbine but also for separating and locating sensitivities inside. In the 7 modified airfoil rows the number of airfoils was reduced by approximately 20%. While the number of airfoils was reduced the axial chord was maintained. Also worksplit, reaction and vortexing were kept constant to concentrate on the pure lift change. In the design phase several Zweifel number levels have been designed showing a straightforward dependence of the efficiency reduction and the Zweifel number increase.

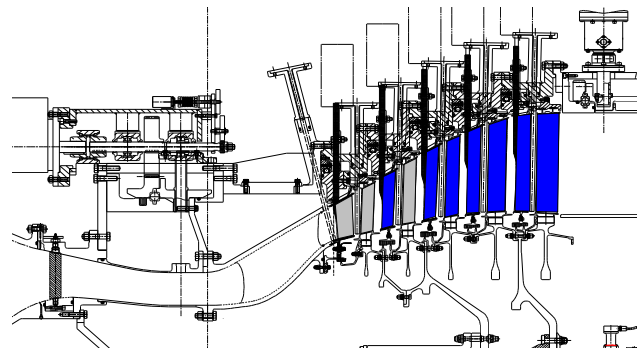


FIG. 9: High lift rig

The rig was tested in the altitude test facility of Stuttgart University. It was heavily instrumented with profile pressures taken on 3 channel heights in all 5 stator rows (FIG. 10). In addition inlet and outlet pressures and temperatures were measured and also measurement were taken between the stages. Finally, a flow visualization with a special dye was performed to evaluate flow structures like separation bubbles.

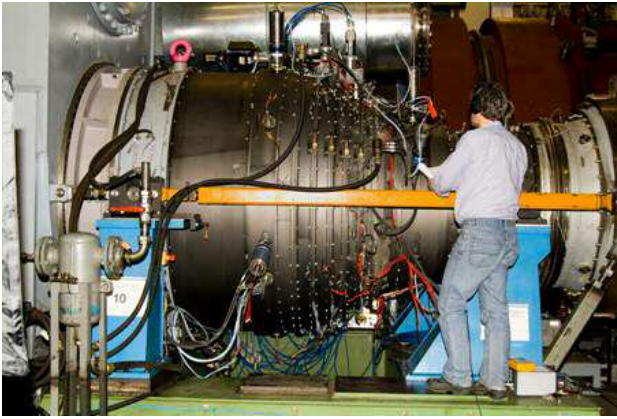


FIG. 10: High Lift rig installed in ATF in Stuttgart

The turbine has been analysed using the 3D CFD solver TRACE routinely used in MTU. In FIG. 11 a comparison is shown between the measured and computed surface pressure distributions of the 3<sup>rd</sup> vane. The general agreement is excellent. And also the small changes in the transition region on the suction side are pretty well captured.

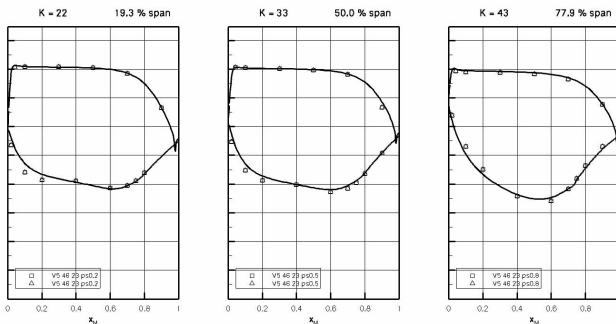


FIG. 11: Comparison of measured and computed pressure distribution in 3<sup>rd</sup> vane for 3 radial locations

The performance impact is evaluated in comparison of the high lift build 2 back-to-back to the conventional build 1 as reference. Since the baseline build 1 features state-of-the-art airfoil designs the comparison gives a reliable and meaningful performance delta. In FIG. 12 this performance delta is plotted for the range of investigated Reynolds numbers. Both builds exhibit the typical Reynolds lapse rate due to the growing effects of viscosity at lower Reynolds numbers. The separation bubble growth seems to be modest for both builds as can be seen through the moderate lapse increase at  $Re < 170k$ .

Comparing the conventional and the high lift build it is interesting to note that the efficiency difference between both builds does not change significantly with Reynolds number. Haselbach et al. [27] actually reported a significant Reynolds lapse increase for the high lift turbine in their investigation. Actually, the measured efficiency difference is slightly larger for the highest Reynolds number. As shown in FIG. 8 the two cascades showed very different Reynolds lapse rates with T162 being quite similar to the reference cascade. A more detailed analysis has to be performed to work out the mechanisms in the modified airfoil rows.

EFFICIENCY CHART

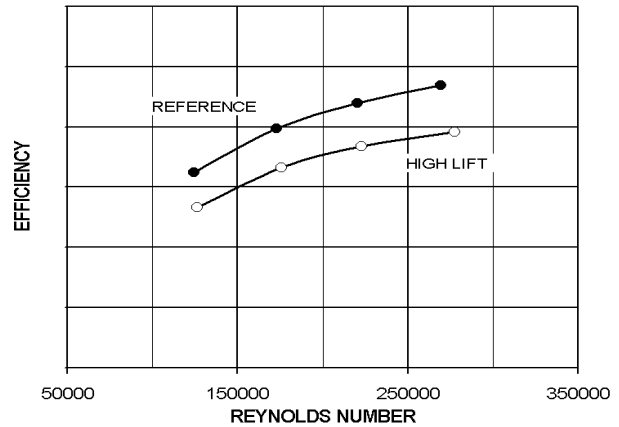


FIG. 12: Efficiency drop as function of Reynolds number (first vane reference)

With these experimental results there is a fundamental basis available for the design of airfoil rows with a point design in terms of airfoil loading especially for mid size to large LP turbines. Due to the good agreement of CFD prediction and measured results the design methodology can be employed to design for airfoil loads, which offer the optimal trade between efficiency, weight and cost issues.

#### 4. THIN SOLID AIRFOIL DESIGN

Solid airfoils are attractive for low pressure turbine airfoil design, because their production cost are significantly lower the cost of hollow airfoils. The main reason is the casting process but also issues like sulfidation protection, which is necessary in the hollow core in some stages. However, due to weight and partially thermo-mechanical fatigue it is not feasible to introduce solid airfoils with a purely aerodynamically optimized thickness distribution. Going to solid airfoils means that the thickness is limited to a value of the order of 2 mm for typical LP turbines leading to thin solid airfoil shapes. Given the high turning levels of around  $100^\circ$  in typical aero engine LP turbines this limitation leads to significant separation bubbles on the pressure side of the airfoils.

The presence of the large pressure side separation bubbles is known to introduce additional losses. A couple of investigations have looked into the flow structure and loss mechanisms in thin airfoils. Gonzalez et al. [35] investigated the combination of high lift and thin solid airfoils in a linear cascade configuration. Brear et al. [36, 37] extended this work and separated the effects at midspan and the secondary flow effects in the endwall region. They found that most of the additional losses occurred close to the endwalls. The influence of the inlet conditions were later discussed by de la Rosa Blanco et al. [38].

Compared to the situation in linear cascades in the absence of radial pressure gradients the situation is even more complicated in real turbines. Due to the radial pressure gradients the flow captured in the pressure separation bubble migrates radially and re-enters the flow in the endwall region. This introduces additional losses in

the following airfoil row through enhanced secondary losses. Overall the additional losses due to pressure side separation bubbles can be significant and can lead to turbine efficiency penalties of the order of 0.5%.

Thus, introducing thin solid airfoils into a low pressure turbine has mainly to be traded between efficiency and cost. In order to improve the trade for thin solid airfoils the concept of partial thickening was tested in a turbine rig build. The concept of partial thickening results from the intention to tackle the major loss increase in the endwall region. By introducing a thickening on the pressure side of thin solid airfoils close to the endwalls an attempt is made to reduce the interaction of the pressure side separation bubble with the secondary flow without a too large weight increase.

The modifications were introduced into a full-scale LP turbine rig, which has 4 rows of thin solid airfoils. In FIG. 13 the three airfoil rows, in which partial thickening was introduced, are shown. The last blade row was omitted, because its pressure side separation bubble was too small to have a significant effect. The partial thickening was designed to only suppress the pressure side separation bubble without effecting the suction side, which is essential for a meaningful comparison.

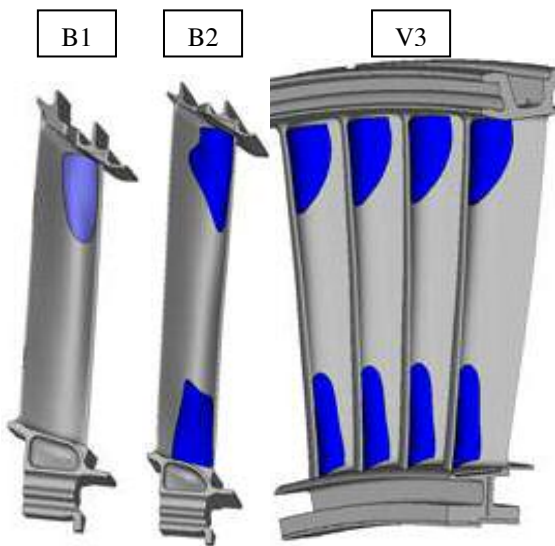


FIG. 13: Thickening region of blade 1 and 2 and vane 3

The rig was heavily instrumented (FIG. 14). Among others, all stator airfoil rows were instrumented, the last two on 5 radial levels. In addition the last rotor row had static pressure installed at midspan. The test was performed in the altitude test facility at Stuttgart University.

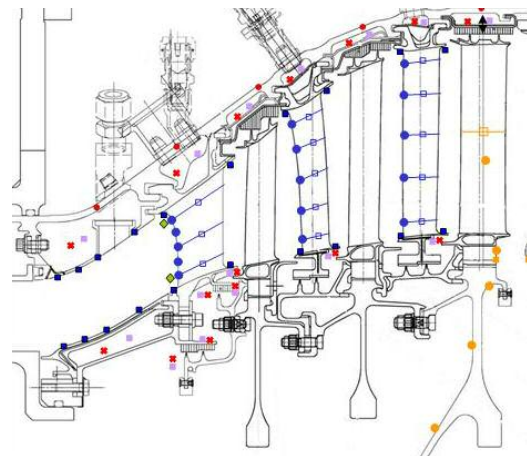


FIG. 14: Three stage LP turbine rig with instrumentation overview.

In FIG. 15 the efficiency is compared between the reference and the partial thickening build for 100% speed. The measured efficiency difference is of the order of 0.2%. The difference is pretty constant over the measured pressure ratio with a slight decrease at high pressure ratio. The reason is the increasing pressure side incidence at high pressure ratios leading to smaller pressure side separation bubbles especially in the rear airfoil rows. The 3D CFD simulation for the same configurations produces a very similar result. Like in the, measurement the efficiency delta slightly decreases for the high pressure ratios. The computed difference between both configurations is of the order of 0.1 to 0.15%, which is a little bit below the measured value but still well within the tolerance bandwidth.

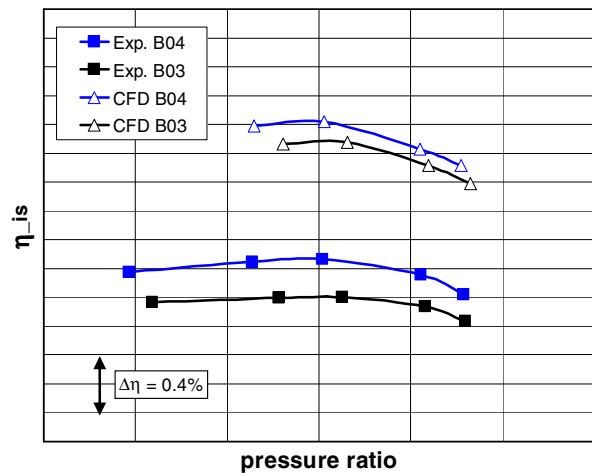


FIG. 15: Comparison of efficiency for reference (B03) and partial thickening build (B04) – measurement and CFD

Finally the radial efficiency distribution is shown in FIG.16. It is obvious that the partial thickening improves the efficiency in the vicinity of the endwalls at the hub and the tip. At midspan the efficiency is unchanged.

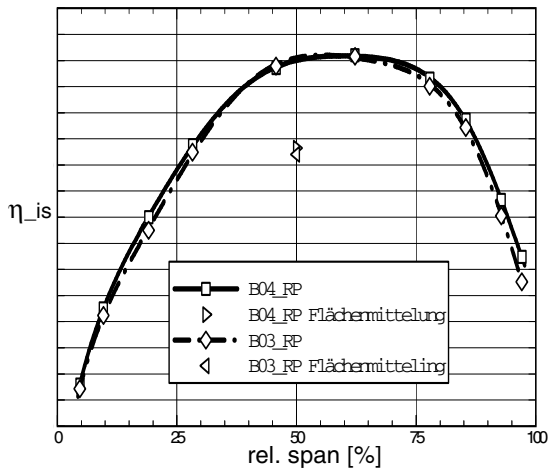


FIG. 16: Radial efficiency distribution for reference (B03) and partial thickening build (B04).

The current investigation shows that partial thickening has the potential to improve the efficiency of thin solid airfoil bladings. This effect can be simulated by 3D CFD, which is important for the design and optimization of low pressure turbine designs with such airfoils.

## 5. NOISE EMISSION

The LP turbine is usually the most important internal noise source in aero-engines after the fan. The high frequency turbine tones are perceived as noisy particularly at the aircraft approach. Therefore the turbine has to be designed in a way that it does not contribute significantly to the overall aircraft noise. To ensure this, accurate noise calculation methods are necessary which are validated by measurements.

To extend the turbine noise database with special emphasis on high speed LP turbines for geared UHBR engines and to evaluate the influence of the speed level, sound measurements have been taken with a 3 stage turbine operated at various speed levels ranging from high speed turbofan to geared UHBR fan engine applications.

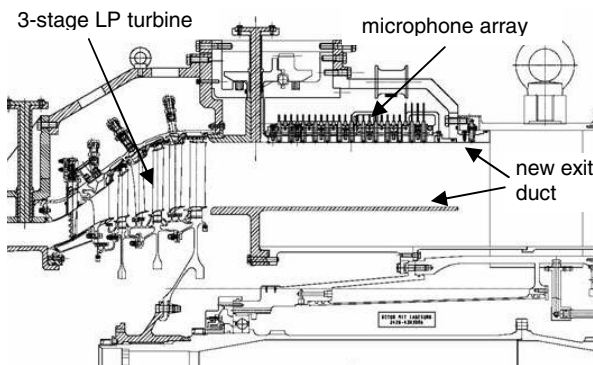


FIG. 17: Turbine rig with sound measurement device

The turbine rig that has been used for the tests is shown in FIG. 17. The sound measurements were taken in close

co-operation with DLR within the EU technology platform SILENCER. A modal measurement technique was applied which has been developed by DLR. This allows to determine the turbine tone noise with better accuracy than analysing engine free-field measurements, as it is not masked by other sources. Additionally, this technique allows to get information on dominating generation mechanisms.

The microphone array in the cylindrical measurement duct at the turbine exit has been designed by DLR. Several configuration variants with different numbers and positions of sensors were studied with respect to maximum frequency, required axial length of the duct section, number of data acquisition channels, measurement time and hardware costs.

The configuration that was finally selected consists of three arrays at evenly spaced azimuthal positions on the outer wall of the rotating duct section, each equipped with 25 flush mounted sensors which are axially spaced by 12.5 mm. This allows an accurate modal analysis up to 7 kHz. The microphones have been mounted on plates along two axial lines of 13 and 12, respectively, see FIG. 18.

During the tests the duct was rotated in steps of 2 degree. Consequently, each measurement was taken at 180 circumferential and 25 axial positions, corresponding to a total amount of 4500 sound measurement positions.

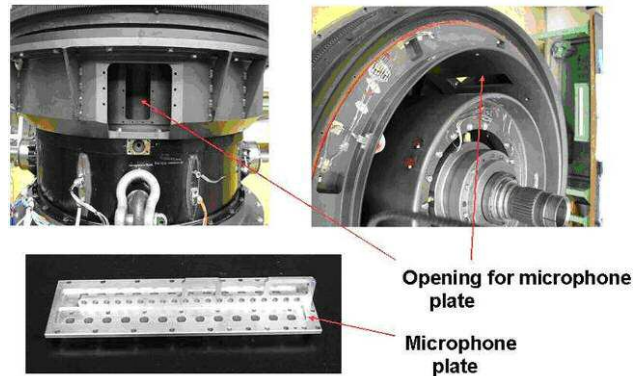


FIG. 18: Turbine rig exit flow duct with microphone plates

The sound data were analysed by DLR to get engine order spectra and thus the complex sound pressures of the dominant tones at all measurement positions. Then the sound data was further processed to get the amplitudes of the upstream and downstream travelling duct modes. Also the modal sound powers were calculated. The powers of the azimuthal modes can be determined by summing up the powers of their radial components and the total sound powers of the tones by summing up the powers of all duct modes.

The test matrix included operating conditions at three speed levels covering the regime from high speed turbofans (operating line 1) to geared UHBR engine applications (operating line 3), see FIG. 19. Previous aerodynamic calculations had shown that the test turbine could be operated at the high speed levels without problems.

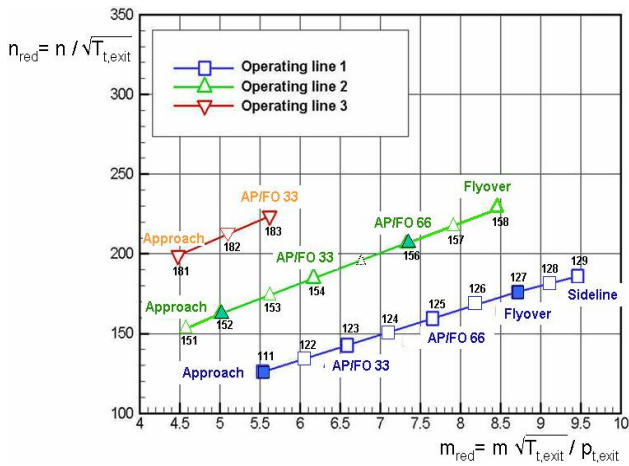


FIG. 19: Turbine test matrix

As a major test result, the downstream propagating corrected sound powers of the BPF tones are plotted vs. the corrected mechanical turbine power in Fig. 20 for the three operating lines. It is seen that, compared on a constant turbine power basis, the influence of the speed level is rather low except for the highest speed level, where the turbine is operated quite far from design.

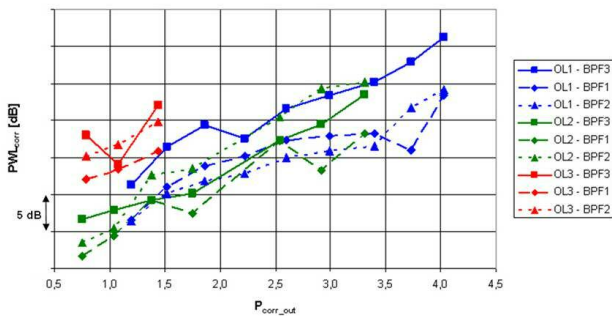


FIG 20: Corrected sound power levels of BPF (blade passing frequency) tones vs. corrected turbine power

Additionally in FIG. 21 the maps of the azimuthal modes propagating downstream are shown for the three blade passing frequency tones at the operating line 1 approach condition, as an example. The experimental results are in good agreement with the theory of Tyler & Sofrin [39]: all dominant modes are rotor / stator interaction modes, whose azimuthal orders can be determined from the blade and vane counts. At the BPF1 tone the dominant mode is -10. It is generated by the interaction between R1 and S2. The mode +6 at the same BPF results from the interaction between R1 and S1. The modal content of the BPF2 tone is dominated by the mode -8, which arises from the interaction between R2 and S2. At BPF3 the dominant mode is -6, which is generated by the interaction between R3 and S3.

Before the tests, sound predictions had been generated with a 3D linearised Euler method and associated tools [40, 41]. Viscous wake interaction and potential flow field interaction with the upstream and downstream cascades have been taken into account. Considerable differences between predicted and measured levels have been observed particularly at the approach operating condition. A potential reason for these deviations is the inaccuracy of the loss factors which determine the amplitudes of the

viscous wakes, particularly at low power conditions where the flow triangles are much different from design.

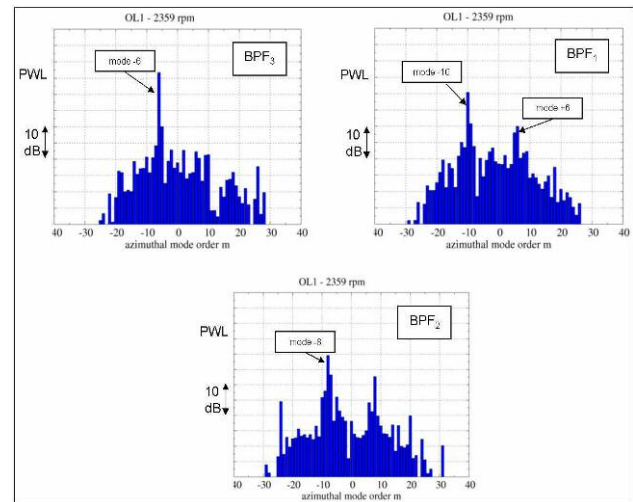


Fig. 21: Maps of the azimuthal modes at operating line 1 approach condition

Generally, the calculations indicated that all three interaction mechanisms generate sound power levels in the same order of magnitude and have therefore to be taken into account. Also it has been found that the propagation of the sound from the generating cascade to the turbine exit has to be taken into account.

## 6. SUMMARY

In this paper a number of measures for improving the environmental friendliness and affordability of future aircraft engines has been presented. All of them require a systematic approach in order to prepare the technological basis up to a technology readiness level sufficient for timely introduction into a new engine. All four projects have in common that based on specific conceptual preparation a final full-scale turbine rig test is being carried out. In all cases the experimental results are employed for a more profound and reliable basis of the design tools ranging from highly empirical ones to sophisticated 3D CFD.

Three-dimensional design for improved efficiency is absolutely necessary for future engines and even after this project is finished work will have to continue. Next generation engines will have an airfoil lift level and distribution specifically designed and optimized for the current application. The high lift work described in this paper together with related experience prescribes a valuable basis for new turbine designs. The application of thin solid airfoils in next generation turbines will depend on the efficiency vs. cost trades and partial thickened airfoils will be considered. And the learning from the extensive noise measurements will help to improve the complicated noise evaluation of new designs and thus enable a much more reliably silent design. Thus, these four projects significantly contribute to the technological advancement in future aero engine low pressure turbines.

## 7. ACKNOWLEDGEMENT

The authors gratefully acknowledge the substantial contributions of people from MTU, ETH-Zürich (LSM), University of Stuttgart (ILA) and University of Federal Armed Forces Munich (ISA). Furthermore the authors would like to thank for the partial funding of the projects through the Luftfahrtforschungsprogramm Phase 3 and the SILENCER program (contract No. G4RD-CT-2001-00500) in the 5<sup>th</sup> European Framework. Finally the authors thank MTU Aero Engines for the permission to publish this work.

## 8. LITERATURE

- [1] Langston, L.S., Nice, M.L., and Hooper, R.M., 1976, "Three-Dimensional Flow Within a Turbine Cascade Passage," ASME Paper No. 76-GT-50
- [2] Pioske, C., 1999, "3D-Gestaltungskonzepte für Turbinenleiträder unter besonderer Berücksichtigung des Sekundärströmungsverhaltens", PhD thesis RWTH Aachen
- [3] Duden, A., Raab, I., & Fottner, L., 1998, "Controlling the Secondary Flow in A Turbine Cascade by 3D Airfoil Design and Endwall Contouring," ASME Paper 98-GT-72
- [4] Sauer, H., Müller, R.; Vogeler, K., 2000, "Reduction of Secondary Flow Losses in Turbine Cascades by Leading Edge Modifications at the Endwall," ASME-paper 2000-GT-0473
- [5] Ardey, S., Gier, J., 2001, "Randzonenbeeinflussung bei Schaufelzahlreduktion in Niederdruckturbinen", DGLR-2001-206
- [6] Eymann, S., Reinmüller, U., Niehuis, R., Förster, W., Beversdorff, M., Gier, J., 2002, "Improving 3D Flow Characteristics in a Multistage LP Turbine by means of Endwall Contouring and Airfoil Design Modification Part 1: Design and Experimental Investigation", ASME-Paper GT-2002-30352
- [7] Gier, J., Ardey, S., Eymann, S., Reinmüller, U., Niehuis, R., 2002, "Improving 3D Flow Characteristics in a Multistage LP Turbine by means of Endwall Contouring and Airfoil Design Modification Part 2: Numerical Simulation and Analysis", ASME-Paper GT-2002-30353
- [8] Harvey, N.W., Rose, M.G., Taylor, M.D., Shahpar, S., Hartland, J., Gregory-Smith, D.G., 2000, "Nonaxisymmetric Turbine End Wall Design: Part I Three-Dimensional Linear Design System," ASME J. of Turbomachinery, Vol.122, pp.278-285
- [9] Hartland, J.C., Gregory-Smith, D.G., Harvey, N.W., Rose, M.G., 2000, "Nonaxisymmetric Turbine End Wall Design: Part II- Experimental Validation," ASME J. of Turbomachinery, Vol.122, pp. 286-293
- [10] Rose, M.G., Harvey, N.W., Seaman, P., Newman, D.A. and McManus, D., 2001, "Improving the Efficiency of the Trent 500 HP Turbine Using Non-Axisymmetric End Walls: Part II Experimental Validation," ASME Paper No. 2001-GT-0505.
- [11] Nagel, M.G. and Baier, R.D., 2003, "Experimentally Verified Numerical Optimization of a 3D-Parameterized Turbine Vane With Non-Axisymmetric End Walls," ASME Paper No. GT2003-38624.
- [12] Ingram, G., Gregory-Smith, D.G., Harvey, N.W., 2004, "Investigation of a Novel Secondary Flow Feature in a Turbine Cascade with End Wall Profiling," ASME Paper GT2004-53589.
- [13] Germain T., Nagel M., Baier R.-D., 2007, "Visualisation and Quantification of Secondary Flows: Application to Turbine Bladings with 3D-Endwalls", Paper ISAIF8-0098, Proc. of the 8th Int. Symposium on Experimental and Computational Aerothermodynamics of Internal Flows, Lyon, July 2007
- [14] Behr, T., Kalfas, A.I., Abhari, R.S., 2007, "Unsteady Flow Physics and Performance of a One-and-1/2-Stage Unshrouded High Work Turbine", ASME J. of Turbomachinery, 129 (ASME Paper No. GT2006-90959)
- [15] Behr, T., Porreca. L., Mokulys, T., Kalfas, A.I., Abhari, R.S., 2006, "Multistage Aspects and Unsteady Flow Effects of Stator and Rotor Clocking in an Axial Turbine with Low Aspect Ratio Blading" ASME J. of Turbomachinery, 128, pp. 11-22.
- [16] Praisner, T.J., Allen-Bradley, E., Knezevici, D.C., Sjolander, S.A., Grover, E.A., 2007, "Application of Non-Axisymmetric Endwall Contouring to Conventional and High-Lift Turbine Airfoils", ASME Paper GT2007-27579
- [17] Entlesberger, R.-G., 2005, Institut für Strahlantriebe, University of Federal Armed Forces Munich, Internal Communications
- [18] Schuepbach, P., 2007, Swiss Federal Institute of Technology, Internal Communications
- [19] Hourmouziadis J., 1989, "Aerodynamic Design of Low Pressure Turbines", AGARD Lecture Series, 167.
- [20] Schulte, V., Hodson, H. P., 1996, "Unsteady Wake-Induced Boundary Layer Transition in High Lift LP Turbines," ASME Paper No. 96-GT-486.
- [21] Gier, J., Ardey, S., Heisler, A., 2000, "Analysis of Complex Three-Dimensional Flow in a Three-Stage LPT by means of Transitional Navier-Stokes Simulation", ASME-Paper 2000-GT-0645
- [22] Ardey, S., Gier, J., Hübner, N., 2000, "Kostenreduktion durch neue aerodynamische Konzepte bei Niederdruckturbinen", DGLR Jahrbuch 2000, pp. 531-539
- [23] Stadtmüller, P., Fiala, A., Fottner, L., 2000, "Experimental and Numerical Investigation of Wake-Induced Transition on a Highly Loaded LP Turbine at Low Reynolds Numbers", ASME paper 2000-GT-269
- [24] Howell, R.J., Ramesh, O.N., Hodson, H.P., Harvey, N.W., Schulte, V., 2001, "High Lift and Aft-Loaded Profiles for Low-Pressure Turbines", ASME J. of Turbomachinery, Vol. 123, pp.181-188.

- [25] Gier, J., Ardey, S., 2001, "On the Impact of Blade Count Reduction on Aerodynamic Performance and Loss Generation in a Three-Stage LP Turbine", ASME-Paper 2001-GT-0197
- [26] Ardey, S., Gier, J., 2001, „Randzonenbeeinflussung bei Schaufelzahlfreduktion in Niederdruckturbinen“, DGLR-2001-206
- [27] Haselbach, F., Schiffer, H.P., Horsmann, M., Dressen, S., Harvey, N.W., Read, S., 2002, "The Application of Ultra High Lift Blading in the BR715 LP Turbine", ASME J. of Turbomachinery, Vol. 124, pp. 45–51, No 1.
- [28] Howell, R. J., Hodson, H. P., Schulte, V., Stieger, R. D., Schiffer, H. P., Haselbach, F., Harvey, N.W., 2002, "Boundary Layer Development in the BR710 and BR715 LP Turbines – The implementation of High Lift and Ultra-High-Lift Concepts", ASME J. of Turbomachinery, Vol.124, pp. 385–392.
- [29] Houtermans, R., Coton, T., and Arts T., 2003, "Aerodynamic Performance of a Very High Lift LP Turbine Blade with Emphasis on Separation Prediction," ASME paper, GT-2003-38802.
- [30] Zhang, X.F., Vera, M., Hodson, H., Harvey, N., 2005, "Separation and Transition Control on an Aft-loaded Ultra-High-Lift LP Turbine Blade at Low Reynolds Numbers: Low-Speed Investigation", ASME paper GT2005-68892
- [31] Vera, M., Zhang, X.F., Hodson, H., Harvey, N., 2005, "Separation and Transition Control on an Aft-Loaded Ultra-High-Lift LP Turbine Blade at low Reynolds Numbers: High-Speed Validation", ASME paper GT2005-68893
- [32] Popovic, I., Zhu, J., Dai, W., Sjolander, S.A., Praisner, T. Grover, E., 2006, "Aerodynamics of a Family of Three Highly Loaded Low-Pressure Turbine Airfoils: Measured Effects of Reynolds Number and Turbulence Intensity in Steady Flow", ASME paper GT2006-91271
- [33] Praisner, T.J., Allen-Bradley, E., Knezevici, D.C., Sjolander, S.A., Grover, E.A., 2007, "Application of Non-Axisymmetric Endwall Contouring to Conventional and High-Lift Turbine Airfoils", ASME Paper GT2007-27579
- [34] Lazaro, B.J., Gonzalez, E., Vazquez, R., 2007, "Unsteady Loss Production Mechanisms in Low Reynolds Number, High Lift, Low Pressure Turbine Profiles", ASME Paper GT2007-28142
- [35] González, P.; Ulizar, I.; Hodson, H. P., 2001, „Improved Blade Profiles for High Lift Low Pressure Turbine Applications“, Proceedings of 4th European Conference on Turbomachinery Fluid Dynamics and Thermodynamics, pp. 129-138
- [36] Brear, M.J., Hodson, H.P., Harvey, N.W., 2001, "Pressure Surface Separations in Low Pressure Turbines: Part 1 of 2 – Midspan Behaviour", ASME paper No 2001-GT-0437
- [37] Brear, M.J., Hodson, H.P., Gonzalez, P., Harvey, N.W., 2001, "Pressure Surface Separations in Low Pressure Turbines: Part 2 of 2 – Interactions with the Secondary Flow", ASME paper No 2001-GT-0438
- [38] de la Rosa Blanco, E., Hodson, H.P., Vazquez R., and Torre, D., 2003, "Influence of the state of the inlet endwall boundary layer on the interaction between the pressure surface separation and the endwall flows", ImechE Journal of Power and Energy. Vol 217 Part A.
- [39] J.M. Tyler, T.G. Sofrin: Axial Flow Compressor Noise, SAE Transactions 70, 1962
- [40] D. Korte, T. Hüttl, F. Kennepohl, K. Heinig: Numerical simulation of multi-stage turbine sound generation and propagation, Aerospace Science and Technology Vol. 9 (2005)
- [41] F. Kennepohl, G. Kahl, K. Heinig: Turbine blade / vane interaction noise: Calculation with a 3D time-linearised Euler method, AIAA-2001-2152